2024-01-2936 Published 12 Jun 2024

# On Improving CLEAN-SC Maps in the Wind Tunnel

**Christof Puhle, Andy Meyer, and Dirk Döbler** GFaI e.V.

***Citation:*** Puhle, C., Meyer, A., and Döbler, D., "On Improving CLEAN-SC Maps in the Wind Tunnel," SAE Technical Paper 2024-01-2936, 2024, doi:10.4271/2024-01-2936.

Received: 16 Feb 2024 Revised: 14 Mar 2024 Accepted: 25 Mar 2024

## Abstract

When traveling in an open-jet wind tunnel, the path of an acoustic wave is affected by the flow causing a shift of source positions in acoustical maps of phased arrays outside the flow. The well-known approach of Amiet attempts to correct for this effect by computing travel times between microphones and map points based on the assumption that the boundary layer of the flow, the so-called shear layer, is infinitely thin and refracts the acoustical ray in a conceptually analogy to optics. However, in reality, the turbulent nature of both the not-so-thin shear layer and the acoustic emission process itself causes an additional smearing of sources in acoustic maps, which in turn causes deconvolution methods based on these maps – the most prominent example being CLEAN-SC – to produce certain ring effects, so-called halos, around sources. In this paper, we intend to cast some light on this effect by describing our path of analyzing/circumventing these halos and how they are linked to the CLEAN algorithm itself. Moreover, we outline a methodological extension to CLEAN-SC, which comes at a reasonable computational cost but effectively eliminates this effect in real-world measurements.

## Keywords

Signal processing, beamforming, acoustic maps, wind tunnel

## 1. Introduction

For many years now, beamforming has been a widely accepted and robust acoustic source mapping technique when using microphone arrays with a limited number of sensors. In very broad terms, it can be described to work as a spatial sound receiver that smoothly either filters out or favors sound emanating from map locations. In the frequency domain, this so-called conventional beamforming produces maps that exhibit only low spatial resolution together with a limited dynamic range. This is especially true for measurements in an open-jet wind tunnel. Therefore, these maps are often subject to further post-processing or deconvolution procedures like CLEAN-SC or DAMAS &c (see [1, 2]). However, these techniques come with assumptions and limitations, which in turn can lead to artifacts making the interpretation of these maps more difficult. This article intends to investigate and effectively eliminate one class of these artifacts that limits the usage of CLEAN-SC.

## 2. Deconvolution of Beamforming Maps Using Clean-SC

Suppose there are $M$ microphones in a phased array with measurable complex sound pressures $p_1, \ldots, p_M \in \mathbb{C}$. The array cross spectral matrix $C \in \mathbb{C}^{M \times M}$ of these signals is composed by the elements

$$C_{ij} = \mathbb{E}\left[p_i p_j^*\right], \tag{1}$$

where $\cdot^*$ denotes complex conjugation, and $\mathbb{E}[\cdot]$ is expectation. Now, given an arbitrary steering vector $g$ associated to a map point, the value $b(g)$ of the conventional beamforming map at this point is

$$b(g) = g^H C g \tag{2}$$

where $g^H$ denotes the conjugate transpose of $g$. There are many definitions of steering vectors in the literature, all of which have their strengths and weaknesses (see [3]). Since the majority of them are based on the travel times between the microphones and the corresponding map point, they allow for a compensation of the flow in an open-jet wind tunnel (see [4, 5, 6, 7]).

Assuming that the conventional beamforming map is a superposition of so-called spatially coherent component maps, CLEAN-SC (see [1]) basically loops over the following steps until a break condition is met: Using the conventional beamforming map initially,

$$C^0 = C,\ b^0(g) = g^H C^0 g, \tag{3}$$

CLEAN-SC begins by determining the maximum $b^i_{max} = b^i\left(g^i_{max}\right)$ of the current map. It then computes the so-called spatially coherent component vector

$$h^i = \frac{1}{b^i_{max}} \cdot C^i g^i_{max} \tag{4}$$

using the current cross spectral matrix. This vector has interesting properties. For example, when computing the following matrix

$$D^i = b^i_{max} \cdot h^i \left(h^i\right)^H, \tag{5}$$

it contains the spatially coherent component of $g^i_{max}$ in $C^i$, i.e.

$$g^H D^i g^i_{max} = g^H C^i g^i_{max} \tag{6}$$

holds for all steering vectors $g$ (of potential map points). In the last step, both the cross spectral matrix and the corresponding map are updated,

$$\begin{aligned} C^{i+1} &= C^i - \varphi \cdot D^i, \quad b^{i+1}(g) \\ &= g^H C^{i+1} g = b^i(g) - \varphi \cdot b^i_{max} \cdot \left|\left(h^i\right)^H g\right|^2 \end{aligned} \tag{7}$$

preparing the next iteration. Here, the so-called loop gain $\varphi \in (0,1]$ can be used to improve robustness of the algorithm. Moreover, CLEAN-SC keeps track of the source locations and levels found in every iteration in form of a so-called clean map (or result map) and refers to the map updated in the process as the dirty map. There are infinitely many choices for source representations in the clean map. Typically, either an analytic function representative or a scaled version of the spatially coherent map itself is used. Figure 1 gives an example on how two different source representations can effect the overall result map. Common choices for break conditions include reaching a maximum number of iterations or a certain limit of dynamic below the first maximum found. Additionally, checking the condition

$$\|C^{i+1}\| < \|C^i\| \tag{8}$$

ensures that the current cross spectral matrix still contains enough information for the loop to continue (see [1]).

For the sake of convenience and clarity, we presented CLEAN-SC using the full cross spectral matrix. In case the diagonal is removed from the CSM, the algorithm follows the same reasoning but equations 4 and 5 have to be adapted for equation 6 to hold (cf. [1] for details).

## 3. Measurement and Halo Effect

The exemplary open-jet wind tunnel measurement used throughout this paper dates back to November 2015. The measurement object was a prototype of a Porsche sports car which was furnished with representative flow-induced sound sources, e.g. a special license plate causing a dominant high-pitch tone.

The measurement was taken using an optimized 3 m × 5 m planar array of gfai tech that consists of $M$ = 192 microphones placed on top of the flow (wind speed 120 km/h) at a distance of 1.8m to the flow. The measurement took 5 s using a sampling frequency of 48 kHz. A fast Fourier transform with prior von Hann weighting was applied to every microphone signal using 50% overlapping blocks of 4096 samples (STFFT). All $192^2$ elements of the array cross spectral matrix (1) were approximated by averaging over these blocks.

On the CLEAN-SC side of things, the loop gain was set to $\varphi$ = 1 and the dynamic range of each frequency coefficient was limited to 60 dB via a break condition. As source representation, a scaled version of the spatially coherent map was chosen. Figure 1 depicts two result maps using different scaling powers.

**FIGURE 1** Representative flow-induced sound sources, CLEAN-SC without diagonal, rows show 2500 Hz (top) and 5000 Hz (bottom) third octave bands, columns show different source representations, sound pressure level, map scale 25 dB

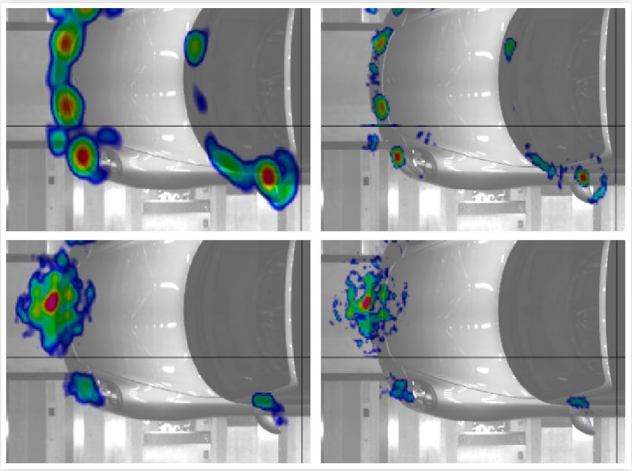

When inspecting these maps more closely, one realizes, that around each main source there exists a silent halo. These halos become even more pronounced, when the main lobe of the source representation is smaller due to a higher scaling power used in the process. Moreover, each of the dominant sources is surrounded by satellite sources which are difficult to interpret as they could simply be remnants of the main source left over by CLEAN-SC in this regard. In the most extreme case of the license plate source, even these satellite sources seem to exhibit the halo effect themselves.

# 4. Investigation and Alternative Methods

In the process of investigating the halo effect, several alternative methods and improvements to CLEAN-SC have been researched. The most promising and insightful ones preceding our proposed solution (see section 5) will be discussed in this section.

## 4.1. Block-by-block Approach

One of the most naive approaches to investigate the effect is to create maps in terms of the smallest time unit used (read: each STFFT block) and to average these maps afterwards. This reveals the turbulent acoustical setting, as – even when CLEAN-SC is used for each block map – sources in the resulting average map appear with a much broader beam width when compared to the standard CLEAN-SC map (see figure 2). Also, source levels are diminished to some extend and dynamic range is lost in comparison to standard CLEAN-SC. However, the halo effect together with the occurrence of satellite sources completely disappeared. On the downside, this method comes at a high computational cost as it directly scales with the number $N = 115$ of STFFT blocks.

## 4.2. Adaptive Beamforming Based Methods

Next, we were interested in whether a completely different method, based on the regular averaged cross spectral matrix, can reproduce the halo/satellite features of standard CLEAN-SC maps. Being one of the most powerful beamforming algorithms, we chose Adaptive Beamforming (see [8]) for this objective; in the one-parameter family of Power Beamforming this corresponds to the case $p = -1$ (see [9]). When applied to our exemplary measurement Adaptive Beamforming produces the maps of figure 3. For lower frequencies they are very similar when compared to block-by-block CLEAN-SC but only come at the computational cost of conventional beamforming ($p = 1$). Again, the halo effect together with the occurrence of satellite sources is not noticeable at all, but, for lower frequencies in particular, sources are not as sharply mapped as in the case of standard CLEAN-SC. Also, the edges of main lobes produced by Adaptive Beamforming appear fuzzy when reaching a certain dynamic in the map.

Although Adaptive Beamforming (by design) is based on the complete cross spectral matrix, i.e. including its diagonal, map dynamics are generally higher than in the case of block-by-block methods without diagonal, but cannot be as high as the ideal dynamics of standard CLEAN maps. Therefore, we implemented a CLEAN algorithm based on Adaptive Beamforming, which in turn lead to the desired map dynamics and exhibits a higher resolution than Adaptive Beamforming (see figure 4).

**FIGURE 2** Representative flow-induced sound sources, standard CLEAN-SC without diagonal (left) vs. block-by-block CLEAN-SC without diagonal (right), rows show 2500 Hz (top) and 5000 Hz (bottom) third octave bands, sound pressure level, map scale 25 dB

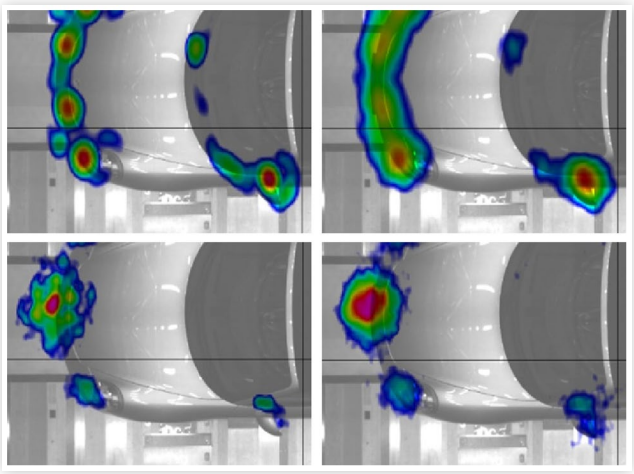

**FIGURE 3** Representative flow-induced sound sources, block-by-block CLEAN-SC without diagonal (left) vs. Adaptive Beamforming (right), rows show 2500 Hz (top) and 5000 Hz (bottom) third octave bands, sound pressure level, map scale 25 dB

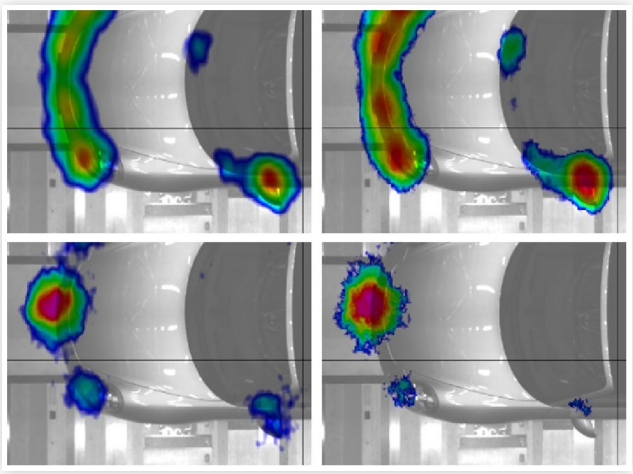

**FIGURE 4** Representative flow-induced sound sources, regular CLEAN-SC without diagonal (left) vs. CLEAN based on Adaptive Beamforming (right), rows show 2500 Hz (top) and 5000 Hz (bottom) third octave bands, sound pressure level, map scale 25 dB

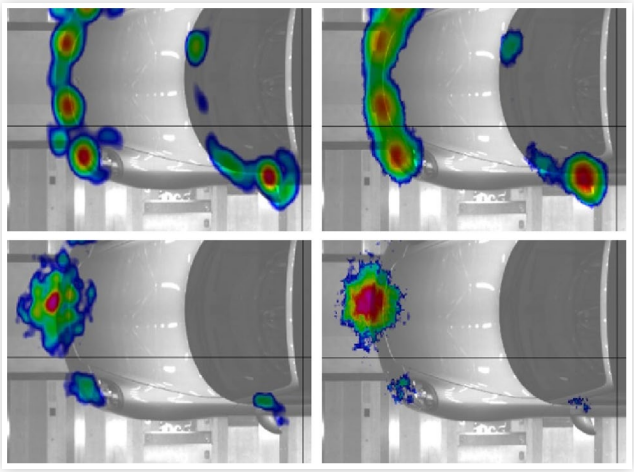

## 4.3. Sub-Array Methods

Another approach that utilizes the regular averaged cross spectral matrix was considered in our investigation: sub-array methods.

Here, a certain number $M'$, or percentage of the total number of microphones $M$ = 192 is chosen randomly leading to a subpar acoustic image with an unusual beam pattern. However, when repeating this process $N' \gg 1$ times and post-processing these images (for example by averaging them), the result is comparable to the block-by-block approach. In figure 5, we present results for $M'$ = 76 (approximately 40% of microphones) and $N'$ = 50

**FIGURE 5** Representative flow-induced sound sources, block-by-block CLEAN-SC without diagonal (left) vs. Conventional beamforming without diagonal of sub-arrays (right), rows show 2500 Hz (top) and 5000 Hz (bottom) third octave bands, sound pressure level, map scale 25 dB

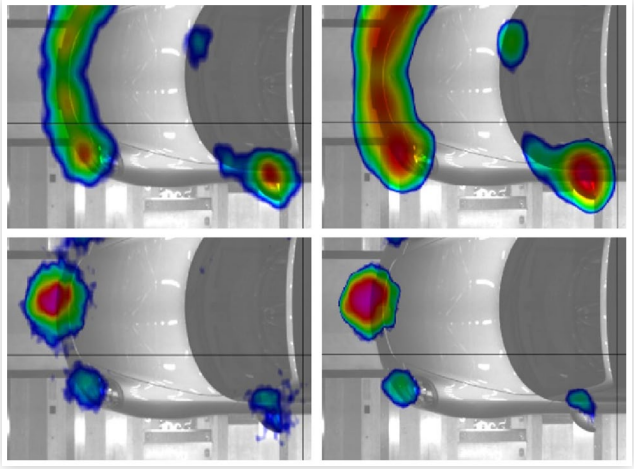

using conventional beamforming without diagonal for each map. Again, the halo/satellite features of the standard CLEAN-SC map are not noticeable. Due to the lower number of microphones $M' < M$ and the lower number of processing steps $N' < N$ and the algorithm used for each map, the computational cost of this sub-array result was significantly lower than the cost of block-by-block CLEAN-SC without diagonal it is contrasted with in figure 5. Moreover, the dynamic range of maps is higher in case of the sub-array approach in this comparison.

# 5. Proposed Method and Results

As a result of our investigations in the previous section, we conclude that the halo effect is – at least for the most part – an artifact of the CLEAN-SC algorithm itself caused by the turbulent components in the acoustic transport processes between sources and microphones. When going back to the equations of section 2, our main observation is that the sole purpose of the dirty map in the iteration is to determine value $b^i_{max}$ and location $g^i_{max}$ of the maximum. However, in principle, the algorithm would still work when not choosing the maximum, or when updating the dirty map in a slightly different manner and therefore separating/uncoupling the two updates of equation 7 from each other. We decide for the latter and remove a modified version $\overline{d}^i(g)$ of the spatial coherent component map

$$d^i(g) = \varphi \cdot b^i_{max} \cdot \left| \left(h^i\right)^H g \right|^2 \tag{9}$$

in each iteration. As before, $\varphi$ = 1 denotes the loop gain, $b^i_{max} = b^i\left(g^i_{max}\right)$ the maximum of the current map in the $i$-th CLEAN iteration and $h_i$ is the corresponding spatially coherent component vector as defined in (4).

The main feature in $\overline{d}^i(g)$ we strive for is a broader main lobe, but without the cost of inflating the side lobes. In order to have a unified basis for our broadening approach, we begin by normalizing the co-domain of $d^i$ linearly to a fixed interval $[\varepsilon, 1]$. Here, $\varepsilon \in (0,1)$ is chosen as small as possible but such that the application of the smooth maps

$$\Psi : [\varepsilon,1] \ni x \mapsto -\lambda \ln(x) \in [0,\infty), \quad \lambda \in (0,1) \tag{10}$$

and

$$\sigma : [0,\infty) \ni x \mapsto x^2 \in [0,\infty) \tag{11}$$

result in a finite numeric value, it depends on the underlying data types and numerics in use. We then transform the normalized map via the broadening automorphism

$$\Psi^{-1} \circ \sigma \circ \Psi : [\varepsilon,1] \to [\varepsilon,1] \tag{12}$$

**FIGURE 6** Porsche sports car (prototype), CLEAN-SC without diagonal (left) vs. its proposed modification (right), rows show 2500 Hz (top) and 5000 Hz (bottom) third octave bands, sound pressure level, map scale 25 dB

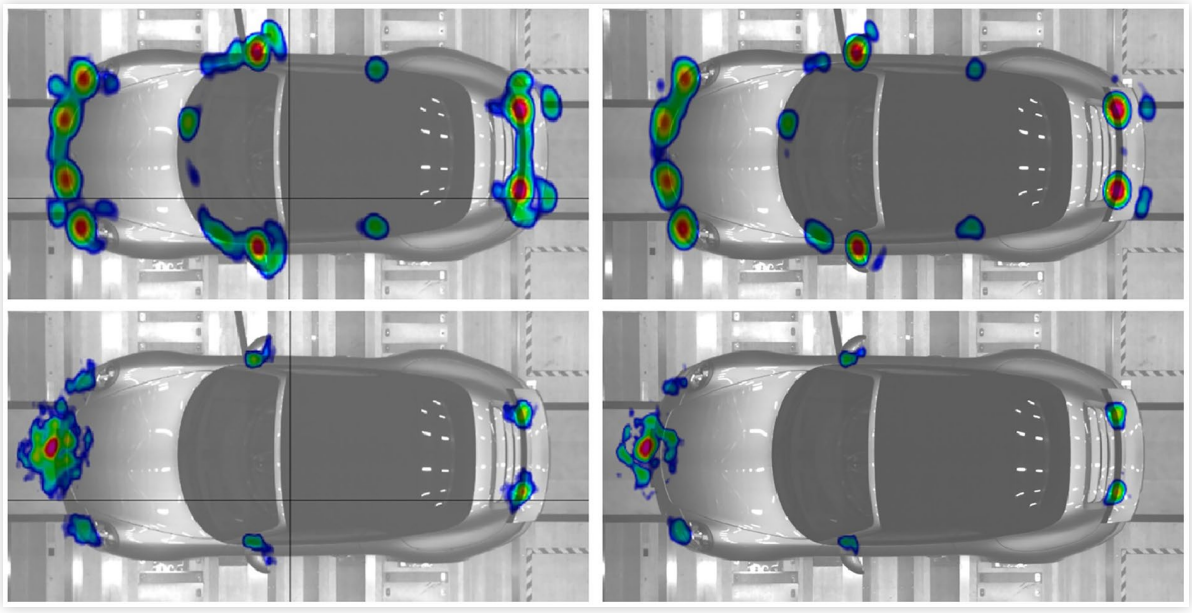

and re-normalize the result to obtain $\overline{d}^{i}(g)$. The role of the control factor $\lambda$ in (10) is a simple result of the interplay between $\Psi$ and $\sigma$ in the automorphism (12). For example, for $x_\lambda := \exp(-1/\lambda)$ we have

$$\Psi^{-1} \circ \sigma \circ \Psi(x_\lambda) = x_\lambda, \tag{13}$$

thus, $x_\lambda$ separates the regions of broadening $(x_\lambda, 1]$ and suppression $[\varepsilon, x_\lambda)$ in (12).

Consequently, the proposed method introduces a new parameter $\lambda \in (0,1)$ to CLEAN-SC, its value has to be chosen depending on the application at hand, in the same way the loop gain $\varphi$ is fixed beforehand. In figure 6, we present results of this CLEAN-SC modification for $\lambda = 0.2$. Since both regular and modified CLEAN-SC loops start with the same conventional beamforming map and use the same source representation procedure, they are directly comparable in terms of source levels, hence will be contrasted to each other in figure 6.

Both, the halo effect together with the occurrence of satellite sources are not noticeable anymore when using the modified CLEAN-SC algorithm. Moreover, the acoustical resolution and beam width of standard CLEAN-SC is preserved. Finally, the computational cost of this modification is comparable to standard CLEAN-SC. Up to now, no non-trivial pitfalls to this method are known to the authors: when balanced right it diminished the halo effect, $\lambda$-values too small overestimate the effect, therefore underestimating real sources in the vicinity of the main lobe under consideration. $\lambda$-values too large could potentially used to remedy an inverse halo effect, thus, $\lambda$ is limited by 1 for our purposes here.

## Acknowledgments

We sincerely thank Jorg Ocker (Porsche AG) and Michael Hartmann (Volkswagen AG) for their constant support and the countless discussions regarding the halo effect.

We especially appreciate the longstanding and close collaboration with Jorg Ocker who brought this problem to our attention and never hesitated to offer his time or measurements in support of its solution.

## Contact Information

puhle@gfai.de

## References

1. Sijtsma, P., "CLEAN Based on Spatial Source Coherence," in *13th AIAA/CEAS Aeroacoustics Conference*, May 21-23, 2007.
2. Brooks, T.F. and Humphreys, W.M. Jr., "A Deconvolution Approach for the Mapping of Acoustic Sources (DAMAS) Determined from Phased Microphone Array," *J. Sound Vib.* 294, no. 4-5 (2006): 856-879.
3. Sarradj, E., "Three-Dimensional Acoustic Source Mapping with Different Beamforming Steering Vector Formulations," *Advances in Acoustics and Vibration* 2012, no. 292695 (2012): 1-12.
4. Amiet, R.K., "Correction of Open Jet Wind Tunnel Measurements for Shear Layer Refraction," American Institute of Aeronautics and Astronautics Paper No. 75-532, 1975.

5. Amiet, R.K., “Refraction of Sound by a Shear Layer,” *Journal of Sound and Vibration* 58 (1978): 467-482.
6. Möser, M., *Messtechnik der Akustik* (Springer, 2010)
7. Ribner, H.S., “Reflection, Transmission and Amplification of Sound by a Moving Medium,” *Journal of the Acoustical Society of America* 29 (1957): 435-441.
8. Johnson, D.H. and Dudgeon, D.E., *Array Signal Processing: Concepts and Techniques* (Prentice Hall, 1993)
9. Puhle, C., “Demonstration of a Unified Approach to Beamforming,” in *Proceedings of 50th International Congress and Exposition on Noise Control Engineering (INTERNOISE 2021)*, Washington, DC, August 2021.



ISSN 0148-7191